The CUE domain of Cue1 aligns growing ubiquitin chains with Ubc7 for rapid elongation

von Delbrueck, M., Kniss, A., Rogov, V.V., Pluska, L., Bagola, K., Loehr, F., Guentert, P., Sommer, T., Doetsch, V.

Molecular Cell
2016 JUN 16 ; 62(6): 918-928
doi: 10.1016/j.molcel.2016.04.031
Publisher: Cell Press / Elsevier

The CUE domain of Cue1 aligns growing ubiquitin chains with Ubc7 for rapid elongation

Maximilian von Delbrück[1,5], Andreas Kniss[2,5], Vladimir V. Rogov[2], Lukas Pluska[1], Katrin Bagola[4], Frank Löhr[2], Peter Güntert[2], Thomas Sommer[1,3*] and Volker Dötsch[2*]

[1] Max-Delbrück Center for Molecular Medicine, Robert-Rössle-Str. 10, 13125 Berlin-Buch, Germany

[2] Institute of Biophysical Chemistry and Center for Biomolecular Magnetic Resonance, Goethe University, Max-von-Laue Str. 9, 60439 Frankfurt am Main, Germany

[3] Institute for Biology, Humboldt Universität zu Berlin

[4] Ludwig Institute for Cancer Research, University of Oxford, Old Road Campus Research Building, Oxford, OX3 7DQ, United Kingdom

[5] These authors contributed equally to this work

* corresponding authors

SUMMARY

Ubiquitin conjugation is an essential process modulating protein function in eukaryotic cells. Amazingly, little is known how the progressive assembly of ubiquitin chains is managed by the responsible enzymes. Only recently ubiquitin binding activity has emerged as an important factor in chain formation. The Ubc7 activator Cue1 carries a ubiquitin binding CUE domain, which substantially stimulates K48-linked polyubiquitination mediated by Ubc7. Our results from NMR-based analysis and *in vitro* ubiquitination reactions point out that two parameters accelerate ubiquitin chain assembly: the increasing number of CUE binding sites and the position of CUE binding within a growing chain. In particular interactions with a ubiquitin moiety adjacent to the acceptor ubiquitin facilitate chain elongation. These data indicate a mechanism for ubiquitin binding in which Cue1 positions Ubc7 and the distal acceptor ubiquitin for rapid polyubiquitination. Disrupting this mechanism results in dysfunction of the ERAD pathway by a delayed turnover of substrates.

INTRODUCTION

Ubiquitination is a crucial post-translational modification involved in many cellular processes. Ubiquitin molecules are transferred to client proteins through the concerted actions of ubiquitin activating enzymes (E1), ubiquitin conjugating enzymes (E2) and ubiquitin ligases (E3). Ubiquitin itself can be targeted for ubiquitination on seven internal lysine residues and on its N-terminus resulting in the assembly of polymeric chains. Distinct chain types do not only display different topologies (Komander & Rape, 2012) but are also associated with divergent signaling output. For instance, polyubiquitin chains linked via K48 represent the major signal for proteasomal degradation (Thrower et al., 2000), while K63-linked chains mediate widespread nonproteasomal functions such as DNA repair, transcriptional activation, endocytosis or protein trafficking (Conaway et al., 2002; Haglund, K., and Dikic, I., 2005; Huang & D'Andrea, 2006; Chen & Sun, 2009). These various polyubiquitin chains are decoded into cellular responses by ubiquitin binding domains (UBD) which guide effector proteins to ubiquitinated substrates (Weissman, 2001). UBDs specifically distinguish between different polyubiquitin molecules by recognizing the linkage and length of chains. Monoubiquitin is bound by UBDs with a K_D in the micromolar range, whereas polyubiquitin chains provide multiple binding surfaces thus increasing binding affinity (Husnjak & Dikic, 2012).

In contrast to this well-known deciphering function of UBDs the function of ubiquitin binding in polyubiquitin chain formation is poorly understood. For instance, activities of the E2 enzymes Ubc13 (Pastushok et al., 2005), Ube2g1 (Choi et al., 2014) and Cdc34 (Choi et al., 2010) rely on ubiquitin binding events. In addition it has already been shown that processive polyubiquitin chain formation can be promoted by noncovalent interactions of ubiquitin with the backside of certain E2 enzymes (Brzovic et al., 2006; Buetow et al., 2015) as well as by RING domains showing ubiquitin binding activity (Brown et al., 2014; Wright et al., 2016).

Furthermore E4 enzymes have been identified that recognize ubiquitinated proteins and elongate the attached ubiquitin chains (Koegl et al., 1999).

A recent report on polyubiquitination activity in the endoplasmic reticulum associated protein degradation (ERAD) pathway revealed that the UBD of Cue1, the CUE domain, stimulates ubiquitin chain formation (Bagola et al., 2013). Cue1 contains a C-terminal Ubc7 binding region (Kostova et al., 2009; Bazirgan & Hampton, 2008) recruiting Ubc7 to the ER membrane (Biederer et al., 1997) for activation (Metzger et al., 2013). Ubc7 acts together with different ERAD RING finger ubiquitin ligases, like HRD1, DOA10 and the Asi complexes (Bays et al., 2001; Kreft et al., 2006; Khmelinskii et al., 2014; Foresti et al., 2014). Substrate proteins are then polyubiquitinated and subsequently removed from the ER membrane by an ERAD specific Cdc48 complex. Subsequently, target proteins are escorted by adaptor proteins to the proteasome in the cytosol.

Although polyubiquitin signals play essential roles in many cellular pathways, the molecular basis on how they are generated remains elusive. In contrast to single attachments of ubiquitin to a substrate, building a ubiquitin chain challenges the E1-E2-E3 cascade with multiple conjugation events at the same molecule. This sequential assembly is a spatially dynamic process in which the distal tip of a growing chain constantly changes its relative position to the active site in the E2-E3 complex. In consequence, chain assembly slows down with increasing chain length as shown for example for the APC/C E3 complex (Meyer & Rape, 2014; Wickliffe et al., 2011). To circumvent this problem, auxiliary factors may facilitate chain assembly and ubiquitin binding domains appear to be the key to this process. Here, we provide a detailed molecular mechanism on how a UBD stimulates ubiquitin polymerization. We demonstrate that the CUE domain of Cue1 accelerates elongation of chains by specific binding events that coordinate the spatial arrangement of the E2 Ubc7 with the distal end of nascent chains.

RESULTS

Helices α1 and α3 of the CUE domain bind the hydrophobic patch of ubiquitin.

Thus far, structural studies on the yeast protein Cue1 have been limited to the Ubc7 binding region (U7BR) (Metzger et al., 2013). The importance of the CUE domain for K48-linked ubiquitin chain formation raised the question how ubiquitin binding and ubiquitin chain elongation are functionally connected (Bagola et al., 2013). As a starting point we used NMR spectroscopy to determine the structure of the CUE domain. This analysis unveiled a compact three-helical bundle characteristic for CUE and UBA domains (Figure 1A). Unlike canonical CUE domains, the CUE domain of Cue1 requires a C-terminal extension, which bears two phenylalanine residues for stable folding (Figure 1A, S1a A-F). In particular F108 is an essential part of the hydrophobic core (Figure S1a C).

To study the interactions between the CUE domain and ubiquitin in more detail we performed NMR titration experiments with ^{15}N-labeled CUE domain and unlabeled ubiquitin (Figure S1b A-E). Chemical shift perturbations (CSP) revealed that the most affected residues of CUE are located in the transition of helix α1 to the adjacent α1α2 loop (V73, L76, A77, N79) and in helix α3 (E96, E100, L103) (Figure 1B). The LAP$^{76\text{-}78}$ motif corresponds to the strictly conserved MFP motif of other CUE domains. Quantitative analysis of the peak positions yielded a dissociation constant (K_D) of 152 ± 5 µM (Figure S1b E). Using a reverse experimental set up, we mapped the interaction surface on ubiquitin (Figure 1B). Titration of ^{15}N labeled ubiquitin with unlabeled CUE domain unveiled that binding involves the hydrophobic patch of ubiquitin centered around amino acids L8-I44-V70 and further includes R42, G47 and L71. Notably, the interaction surface on ubiquitin is in close proximity to the K48 residue without K48 directly contributing to binding (Figure 1C).

Based on the chemical shift perturbation pattern we calculated a structural model of the CUE/ubiquitin complex using the software package HADDOCK (de Vries, Sjoerd J et al.,

2010). This model supports a significant contribution of R42 in ubiquitin for the interaction with E100 of CUE (Figure 1C). At the same time this structural arrangement ensures that K48 of ubiquitin is accessible for further chain elongation (Figure S1b F).

Fluorescence-based analysis of ubiquitin chain elongation reactions

Knowing the binding properties of the CUE domain we tried to understand how an interaction with ubiquitin stimulates ubiquitin chain formation by Ubc7. Therefore, we developed a fluorescence-based assay that allows to follow precisely elongation reactions of ubiquitin chains. Different chains of defined linkage and length were used as ubiquitin acceptors. These model substrates were blocked at their C-termini to prevent charging onto enzymes. Elongation of chains by single fluorescently labeled ubiquitin molecules was monitored using fluorescence anisotropy. In elongation experiments with tetraubiquitin the signal increased due to a slower tumbling of the formed pentaubiquitin when compared to labeled monoubiquitin (Figure 1D, 1E). This change in fluorescence anisotropy is strictly dependent on ATP. After subsequent addition of a deubiquitinating enzyme ($Usp2_{cat}$), ubiquitin chains were completely disassembled and fluorescence anisotropy decreased to its original level. Reactions lacking preassembled chains did not show a rise in signal. In addition, elongation of tetraubiquitin was pursued by quantifying fluorescence intensities of the reaction product pentaubiquitin applying gel electrophoresis (Figure 1F, S1c B). Both experimental approaches yielded equivalent kinetics (Figure S1c A) supporting fluorescence anisotropy measurements to be a robust and precise tool to monitor chain elongation. Reaction catalysis required additionally an E1 enzyme (Ube1), the *yeast* E2 enzyme Ubc7 and the soluble fragment of Cue1 (cCue1, residues 25-203) which encompasses both the CUE domain and the U7BR. Some experiments included the cytosolic fragment of the E3 enzyme Hrd1 (cHrd, residues 325-551) containing the RING-finger domain.

Ubiquitin binding affinity correlates with kinetics of chain elongation and substrate degradation

In the absence of cCue1, chain elongation by Ubc7 was strongly impeded (Figure 2B). This observation can be attributed to the missing activation of the E2 enzyme by the U7BR (Metzger et al., 2013). To investigate the impact of the CUE domain on polyubiquitination, the structurally important LAP^{76-78} motif was replaced by RGA^{76-78} (cCue1 RGA; (Bagola et al., 2013)) which results in an unfolded CUE domain (Figure S1a F). Consistent with previously published data, reactions containing cCue1 RGA were substantially impaired for chain elongation (Figure 2B). In the presence of wild type cCue1, elongation of K48-linked tetraubiquitin ($K48\text{-}Ub_4$) was fivefold faster than in the absence of a functional CUE domain, as indicated by the kinetic rate constants (Figure 2D). In line with this acceleration, the presence of a functional CUE domain increased the yield of elongation product (Figure 2F). Chain elongation did not require cHrd1, but was facilitated by addition of the RING domain (Figures 2B, 2C). The U7BR-bound Ubc7 has an increased affinity for its cognate E3 RING domain which in turn promotes discharging of ubiquitin from the E2, thereby driving ubiquitination (Metzger et al., 2013).

Kommentar [b1]: Wir haben auf Seite 6 oben einmal von RING finger domain gesprochen. Ich glaube fortlaufend genügt die Bezeichnung RING domain, um ein paar Zeichen zu sparen.

To investigate whether ubiquitin binding of the CUE domain directly correlates with the propensity of Cue1 to enhance chain elongation, we substituted amino acids in the UBD involved in this interaction. These variants (E96A, E100A and L103A) retained the CUE-fold but weakened ubiquitin binding affinity as determined by NMR titration experiments (Figure 2A, 2E, S2 A-B). While the E96 side chain does not contribute to ubiquitin recognition, binding activity was decreased for the E100A and even more for the L103A variant (as seen from the NMR titration experiments). Testing these cCue1 variants in elongation reactions with tetraubiquitin revealed a consistent correlation between binding affinities and kinetic rate constants. Wild type cCue1 ($(4.87 \pm 0.20) \times 10^{-3}\ s^{-1}$) and the E96A variant ($(4.46 \pm 0.13) \times 10^{-3}\ s^{-1}$) exhibited comparable elongation kinetics. In contrast, reactions containing variants

E100A ((2.13 ± 0.05) $x10^{-3}$ s^{-1}) and L103A ((1.48 ± 0.03) $x10^{-3}$ s^{-1}) were 2-3 fold slower (Figure 2D). Accordingly, the total amount of the reaction product pentaubiquitin was reduced (Figure 2F). Similar effects on elongation kinetics were observed regardless, whether cHrd1 was present or absent (Figure 2C). Finally, we analyzed the Cue1 variants *in vivo* addressing polyubiquitin-mediated protein degradation. Ubc6 is a substrate of the DOA10 ubiquitin ligase complex and as such degraded by proteasomes in a Cue1/Ubc7 dependent manner (Bagola et al., 2013). In line with a slower assembly of ubiquitin chains due to a weaker ubiquitin binding, Cue1 variants delayed the degradation of Ubc6 in yeast while complete absence of Cue1 or Ubc7 had a strong effect since in both cases the conjugating activity is missing (Figure 2G). Thus, a rapid elongation of ubiquitin chains by Ubc7 relies on specific ubiquitin binding events by the CUE domain of Cue1, and seems to be required for the efficient degradation at least of some ERAD substrates.

Ubiquitin chains with K48-linkages and growing length are preferentially elongated by cCue1/Ubc7

Ubc7 exclusively assembles K48-linked polyubiquitin on substrates *in vivo* (Ravid & Hochstrasser, 2007; Choi et al., 2014) and unanchored ubiquitin chains *in vitro* (Bagola et al., 2013). A substrate protein does not seem to be essential for polyubiquitination activity. Elongation reactions of monoubiquitin provide further evidence for a self-contained E2 system with the task to extend ubiquitin chains. All experiments with cCue1/Ubc7 and ubiquitin chains revealed a stimulation of elongation due to the CUE domain. This is in contrast to reactions with monoubiquitin that show no enhancing effect of the UBD (Figure 3A).

To evaluate this function, we applied ubiquitin chains of different linkage and length as substrates in our fluorescence-based assay. Additionally, we examined whether changes in the

kinetics of chain elongation would correlate with differences in the binding affinities of the CUE domain by SPR and NMR experiments. In line with a modestly stronger interaction with K48-linked chains (Figure S3 A-D), we observed preferential elongation of K48- over K63-linked substrates (Figure 3B, 3C, S3E, S3G, S3I). Distal elongation of the latter model substrate was ensured by K48R substitutions in all positions except at the distal ubiquitin. Besides the linkage type of a substrate, its size also influenced the elongation rate (Figure 3B). Increasing chain length accelerated elongation kinetics in the presence of the CUE domain, which can be explained by higher local concentrations of Ubc7 in the surrounding of chains due to more binding sites. This effect is again modestly more pronounced for K48-linked chains than for K63-linked substrates corresponding to the higher affinity of CUE to K48-linked ubiquitin.

cCue1 RGA was employed in kinetic analyses to evaluate the capability of U7BR-bound Ubc7 to elongate chains. Without a functional CUE domain, reactions with cCue1/Ubc7/cHrd1 were remarkably slow (Figure 3D, 3F S3F, S3H, S3J). In line with the general constraint of polyubiquitination lacking auxiliary ubiquitin binding events (Meyer & Rape, 2014; Wickliffe et al., 2011) elongation was decelerated with increasing chain length, an effect more pronounced for K48- than for K63-linked chains. Next, we determined the degree of acceleration caused by the CUE domain to assess its function in chain elongation. The CUE domain specific factor is set as the ratio of kinetic rate constants from reactions with wild type cCue1 to reactions with cCue1 RGA and attained higher values for K48-linked chains than for K63-linked chains (Figure 3E). Moreover, the acceleration increased from K48-linked di- to tetraubiquitin, which was not observed for K63-linked chains. In summary, these results indicate that the CUE domain of Cue1 progressively accelerates elongation of K48-linked chains with increasing length counteracting the inability of Ubc7 to rapidly elongate growing chains.

CUE binds the proximal moiety of K48-linked diubiquitin with higher affinity than the distal molecule

To understand, why the CUE domain shows a small but significant preference for K48-linked chains, we synthesized K48- and K63-linked diubiquitin containing ^{15}N-labeled moieties at either the proximal or distal position. Upon titration with unlabeled CUE domain, binding events at one of both positions could be analyzed. Chemical shift perturbations suggested that the interfaces of interaction with Cue1 are similar on mono- and diubiquitin (Figure 4A-D). However, we observed one interesting difference between the associations to K63- and K48-linked diubiquitin. The latter displayed an additional interaction event involving position G75 at the C-terminus of the distal ubiquitin moiety. Since the K48 residue of ubiquitin is in close proximity to the CUE binding site, this additional interaction specifically results from K48-linked monomers. Employing a binding model assuming two different binding sites in diubiquitin we quantitatively analyzed NMR titration experiments and calculated K_D values (Figure 4E, 4F, S4). In K48-Ub_2 the CUE domain preferentially binds proximal ubiquitin (84 ± 8 µM) approximately twofold tighter than distal ubiquitin (151 ± 13 µM). In contrast, no difference in affinity for distal and proximal binding was detected for K63-linked diubiquitin (~100 µM; Figure 4F). Interestingly a previous study has presented similar binding analyses involving the CUE domain of the mammalian ERAD E3 gp78 revealing a preference for the distal moiety in K48- and K63-linked diubiquitin (Liu et al., 2012) reflecting a different organization in this ubiquitin ligase.

CUE domain binding adjacent to the distal acceptor ubiquitin promotes chain elongation

Finally, we wanted to know whether the influence of the interaction of Cue1 with K48-linked ubiquitin molecules on the chain elongation is position dependent. Thus, we introduced the amino acid exchange R42A in either moiety of diubiquitin (Figure 5A). Monoubiquitin R42A displays reduced binding to the CUE domain (K_D = 600-700 µM, Figure 3C). When placed in the distal molecule that serves as an acceptor for ubiquitin conjugation, the R42A variant had a negligible effect on elongation kinetics. In contrast, R42A at the proximal position reduced elongation in rate and efficiency. These findings suggest that binding of Cue1 to the proximal ubiquitin adjacent to the acceptor site promotes polyubiquitination. Elongation experiments of these diubiquitin molecules in the presence of cCue1 RGA exhibited almost identical reaction kinetics indicating that the observed position effect is CUE domain specific. Moreover, the UBD stimulated reactions in the presence of cHrd1 implying Cue1 to act as a prevalent scaffold for ubiquitin chains (Figure S5A).

We now wondered how CUE binding within longer chains affects the elongation kinetics. K48-Ub_4 variants with single R42A amino acid exchanges in different ubiquitin moieties feature an equal number of binding sites and enabled us to map the action profile of the CUE domain. Again, analysis of chain elongation kinetics yielded the most pronounced effect by introducing the R42A variant adjacent to the distal acceptor ubiquitin (Figure 5B, S5B, S5D). For this substrate the slowest elongation reaction was observed (~70% of wild type rate constant). Introducing multiple R42A ubiquitin variants in Ub_4 decelerated elongation even further (Figure 5C, S5C, S5E). These data suggest that binding of cCue1 to any moiety within the chain accelerates the elongation reaction. However, the degree of stimulation depends on the position of the interaction within a chain, showing the highest impact when placed next to the acceptor ubiquitin. This effect is independent of linkage type and can also be measured for K63 linked diubiquitin (Figure S5F) suggesting that interaction with the ubiquitin molecule next to the acceptor site provides the optimal steric arrangement for Ubc7 based chain elongation.

To validate the importance of the position effect we restricted CUE-ubiquitin interactions to certain positions within a chain. Therefore, we chemically crosslinked the single cysteine variant of cCue1 (T66C, C147S) with different ubiquitin (T9C) moieties (Figure S5G). Crosslinking cCue1 to the proximal moiety in diubiquitin showed a drastic increase of the rate and efficiency of chain elongation (Figure 5D). Chain elongation was slower when cCue1 was crosslinked to the proximal position in triubiquitin. In contrast crosslinking to the distal position of diubiquitin had an inhibitory effect. This strong acceleration of the chain elongation by crosslinking to the positions adjacent to the acceptor site supports our model.

DISCUSSION

Shaping a ubiquitin chain represents an intriguing steric problem. The longer a chain grows, the larger is the distance to the active center of the involved E2-E3 ligase complex. In a stochastic process the growth of ubiquitin chains should slow down with increasing length of a chain. This general constraint in polyubiquitin formation was previously reported (Meyer & Rape, 2014; Wickliffe et al., 2011). It is consistent with our kinetic measurements of the E2 Ubc7 activity missing a functional UBD. Here, we present a mechanism on how the presence of the CUE domain in Cue1 counteracts this effect by directing Ubc7 to acceptor lysine residues at a distal ubiquitin molecule of a nascent ubiquitin chain. This leads to a progressively accelerated elongation reaction with increasing chain length.

Corresponding to the K48-linkage specificity of Ubc7 (Bagola et al., 2013), CUE features a modestly stronger binding to K48-linked ubiquitin assemblies than to other chain types. The preference is caused by additional interactions at the C-terminus of the neighboring ubiquitin molecules in these chains. In consequence, linked moieties in a chain are bound twofold stronger than the distal one. Furthermore, we observed an unconventional binding interface

compared to consensus CUE domains. K48 of ubiquitin is excluded from the binding interface with Cue1 while for instance the CUE domain of Cue2 directly involves K48 thus potentially blocking it for further modifications (Kang et al., 2003). The accessibility of this lysine residue is a prerequisite for chain formation by Ubc7. Consistent with the binding preference, K48-linked chains are elongated faster than K63-linked model substrates in the presence of the CUE domain. However, since the Ubc7 system within ERAD is based solely on K48 linked chains, there was no evolutionary pressure to optimize the system for K48 versus K63 linkage types, explaining the relatively small differences observed for the interaction of the CUE domain with both chain assemblies. In summary, CUE binding converts an inherent decelerating chain formation by Ubc7 into a self-accelerating process.

Based on our kinetic analysis, we suggest two major factors increasing the pace of chain assembly. First, the number of binding sites: Reducing the number of binding sites by introducing specific variants into ubiquitin chains or the CUE domain decelerates elongation reactions. This includes also the acceptor ubiquitin moiety and strongly indicates that multiple interactions of Cue1 with a ubiquitin chain increases the local concentration of Ubc7 which in turn promotes chain elongation.

Second, the position of CUE binding: A deficient binding to the ubiquitin moiety adjacent to the distal end of a chain has a greater impact on the rate of chain assembly then at other positions. In addition crosslinking of cCue1 with ubiquitin at this position enhanced chain elongation most. An interaction of Cue1 with the penultimate ubiquitin in a chain most likely orientates Ubc7 to the distal end of a ubiquitin chain to productively transfer ubiquitin from the charged E2 to the acceptor lysine of the distal moiety. Binding to ubiquitin further away from the distal end shows a diminished stimulation due to an increasing distance from the ubiquitin acceptor molecule.

In comparison to a recently reported mode of chain formation described in cell cycle control, our proposed mechanism seems to be perfectly adapted to rapid proteolytic processes of

substrates with divers biophysical properties, like in the case of the ERAD system (Kelly et al., 2014). The APC/C is a tightly adjusted system for regulatory degradation of cell cycle protagonists and simultaneously coordinates recognition and ubiquitination of a limited pool of defined substrates. Here, the RING domain increases the affinity of the E2 Ube2S to the distal ubiquitin molecule whereby chain elongation is enhanced. Tracking the end of chains is a stimulating effect, which subsides with increasing chain length. ERAD challenges ubiquitin ligases with a much wider range of target proteins, although not all ERAD substrates seem to depend on the presence of a CUE domain (Bagola et al., 2013). In order to achieve rapid removal of substrates with diverse biophysical properties, robust K48-linked chain formation must be guaranteed. In contrast to a self-limiting ubiquitination in cell cycle control, ERAD employs a self-accelerating chain assembly when Cue1 is involved. At the APC/C the contribution of the RING domain in an enhanced polyubiquitination directly connects substrate binding and ubiquitination. In contrast Cue1/Ubc7 may represent a self-contained module, adapted to quickly assemble K48-linked chains on diverse substrates in concert with different ubiquitin ligases. Recognition of certain substrate classes and their cytosolic ubiquitination seems to be disconnected at ERAD ubiquitin ligases. In the case of Hrd1, substrate recognition occurs at the ER-luminal Hrd3 domain of the ligase complex (Carvalho et al., 2006; Denic et al., 2006). This may avoid steric clashes of fixed substrates and growing chains.

Based on our results, we want to propose the following model for a UBD-mediated polyubiquitination by Ubc7 (Figure 6). In a first step, substrate proteins are ubiquitinated on one or several lysine residues. Here, contribution of the CUE domain is probably limited to shield initial modifications from deubiquitinating enzymes (Bagola et al., 2013). As soon as the substrate is primed with diubiquitin, the machinery switches to highly processive chain elongation. Cue1 binds the moiety adjacent to the acceptor ubiquitin and orients Ubc7 for ubiquitin transfer. The preference of the CUE domain for K48-linked molecules enhances this

position effect and keeps the distal ubiquitin accessible. The CUE domain binds individual ubiquitin moieties with low affinity allowing dynamic motions within the growing chain. Since the off-rate of the CUE domain – ubiquitin complex is much faster than the rate of the enzymatic reaction, a higher number of binding sites within the growing chain does not inhibit the overall reaction but accelerates it by keeping the E2 in close proximity to the growing chain and at the same time allowing the system to sample all possible interaction positions efficiently. While the absolute acceleration effects are relatively small (factor 2-5) as compared to typical acceleration effects of enzymatic reactions with small molecules, they are within the same range as observed for other interactions within ubiquitin system (Metzger et al., 2013). The CUE domain enables Cue1 to act in an E4-like fashion by implementing an acceleration factor of chain elongation. Our data suggest that in the absence of a functional CUE domain, ubiquitin chains should be formed less efficiently on specific ERAD substrates. In line with this prediction we found that variants with reduced affinity of the CUE domain delayed proteasomal degradation of the ERAD substrate Ubc6 *in vivo*. Since Ubc6 degradation has also been shown to involve priming of the substrate with K11-linked chains the CUE domain might also contribute to K11-chain extension (Kreft & Hochstrasser, 2011; Xu et al., 2009). Strikingly, decelerated chain synthesis is neither compensated by downstream acting E4 enzymes at the level of Cdc48 nor by the proteasome (Schmidt et al., 2005; Crosas et al., 2006; Jentsch & Rumpf, 2007). Hence, turnover kinetics seem to be directly defined by the efficacy of the primary ubiquitination.

EXPERIMENTAL PROCEDURES

Protein purification for structural and interaction studies

The codon optimized gene of Cue1$^{25-203}$ and related constructs containing only the CUE domain were expressed as polyhistidine tagged ubiquitin fusion proteins (Rogov et al., 2012). Expression was carried out in T7 Express competent *E. coli*. Cells were grown in LB or M9 medium and induced at 18 °C for 20 h with 0.2 mM IPTG. Purification included lysis, Immobilized Metal Affinity Chromatography (IMAC), tag removal by TEV protease, a second IMAC step followed by gel filtration.

To biotinylate the CUE domain a biotinylation site was introduced between the TEV site and the coding sequence of Cue1$^{59-115}$. *In vitro* biotinylation was performed in 50 mM bicine (pH 8.3), 10 mM ATP, 10 mM MgOAc and 50 µM biotin using BirA for 1h at 30 °C.

Protein expression, purification and fluorescence labeling for functional analysis

Ubc7, Hrd1$^{325-551}$ (cHrd1), Cue1$^{25-203}$ (cCue1) and Cue1$^{25-203}$ variants were cloned in a pGEX-6p1 vector, expressed and purified as described before (Bagola et al., 2013). Ube1 subcloned in a pET21d vector was produced according to a published protocol (Berndsen & Wolberger, 2011). Cdc34, Ubc13 and Uev1a in pGEX vector were expressed and processed as previously reported (Mansour et al., 2014). The catalytic domain of the deubiquitinating enzyme Usp2 (Usp2$_{cat}$) was purchased from Boston Biochem. Human ubiquitin (Ub) and all its variants, cloned in pETM60, were expressed in *E. coli* BL21 cells and produced according to previous protocols (Pickart & Raasi, 2005; Mansour et al., 2014). Labeling of cysteine containing ubiquitin variants with the fluorescence dye Alexa Fluor 488 C5 Maleimide has been described (Bagola et al., 2013).

Preparative assembly of ubiquitin chains

Ubiquitin chains with proximal hexahistidine tag (6xHis) were enzymatically assembled *in vitro.* K48-linkages were synthesized using Cdc34, while K63-linked chains were generated by Ubc13 and Uev1a. A detailed description of the reaction conditions is available in Supplemental Experimental Procedures.

NMR spectroscopy

NMR experiments were performed at 298K in NMR buffer (50 mM Na_2HPO_4, 100 mM NaCl, pH 7, 5% D_2O). NMR structure determination of ^{13}C-^{15}N-labeled $Cue1^{45-115}$ followed a standard protocol (see Supplemental Information).

Titration of ^{15}N-labeled ubiquitin with CUE or ^{15}N-labeled CUE (0.2 mM) with Ub or Ub chains was monitored by [^{15}N, ^{1}H]-HSQC spectra. Spectra were acquired at CUE:Ub molar ratios of 0, 1/8, 1/4, 1/2, 1, 3/2, 2, 4, 8 and 16 (only in case of monoubiquitin titration). Since a ubiquitin chain presents multiple binding sites for CUE the molar ratios were accordingly corrected.

The structural model of the CUE/ubiquitin complex was calculated in HADDOCK. Ambiguous interaction restraints (AIR) were defined for solvent accessible amide resonances shifting more than 0.10 ppm under saturation for CUE, and 0.12 ppm for ubiquitin.

K48-Ub_2 (0.2 mM) and K63-Ub_2 (0.2 mM) carrying either a proximal or distal ^{15}N-labeled ubiquitin were titrated with unlabeled $Cue1^{45-115}$ up to a molar ratio of 8. To determine the dissociation constants for proximal and distal ubiquitin moieties a fitting model for two independent binding sites with different affinities was used (Varadan et al., 2005; Wang & Jiang, 1996).

CD spectroscopy

CD spectroscopy experiments were performed using a JASCO J-810 spectropolarimeter (JASCO, USA) in a 0.1 cm pathlength cuvette. Temperature induced unfolding was monitored by ellipticity changes at 222 nm from 4 to 90°C. Protein concentrations were adjusted to 100 µM in NMR buffer.

***In vitro* ubiquitin chain elongation reaction for fluorescence based analysis**

In vitro ubiquitination reactions (performed in triplicates) modified for analysis of ubiquitin chain elongation included 0.15 µM E1 (Ube1), 2 µM Ubc7, 1.2 µM cCue1 or variants, 14.8 µM preassembled ubiquitin chains and 0.2 µM Alexa Fluor 488 labeled Ub in FA buffer (4 mM ATP, 0.5 mM DTT, 4 mM $MgCl_2$, and 50 mM Tris/HCl pH 8). Optionally 1 µM cHrd1 was added. Reactions of time course experiments were performed in the dark at 10 °C containing cHrd1 or at 20 °C omitting the RING fragment. In another set of chain elongation experiments cCue1 was crosslinked to Ub T9C which was integrated either at the distal (K48-Ub_2^{distal}~cCue1) or proximal position (K48-$Ub_2^{proximal}$~cCue1) of diubiquitin or the proximal position of triubiquitin (K48-$Ub_3^{proximal}$~cCue1). Crosslinking reactions with $BM(PEG)_2$ were carried out according to the manufacturer's manual. Conjugates were included in *in vitro* ubiquitination reactions and performed in triplicates. Reactions included 0.15 µM E1 (Ube1), 2 µM Ubc7, 1.2 µM cCue1 T66C C147S crosslinked to Ub T9C (in Ub_2 or Ub_3), 0.2 µM Alexa Fluor 488 labeled Ub in FA buffer. A similar reaction without crosslinked conjugates contained equal amounts of cCue1 and K48-Ub_2 (1.2 µM).

At given time points samples were taken and elongation was stopped using urea sample buffer. Elongation reactions monitored by fluorescence anisotropy were carried out at 20 °C. Polarized emissions at 518 nm after excitation at 495 nm were measured in a

Spectrofluorometer (Fluoromax 4, Horiba). For subsequent deubiquitination 500 nM $Usp2_{cat}$ was added after saturation of chain elongation.

Elongation products were analyzed by SDS-PAGE following fluorescence scanning employing emission filter LPB (510LP) after excitation at 473 nm and Coomassie Brilliant Blue staining.

Fluorescence intensities of elongation products were quantified using ImageQuant TL software and normalized to total fluorescence signals. Single exponential elongation kinetics were analyzed with FluorEssence™ Software and SigmaPlot Version 12 yielding kinetic rate constants of elongation reactions.

SPR studies

SPR experiments were performed on a Biacore X100 system. Biotinylated CUE was immobilized (~100 RU) on a streptavidin coated sensor chip. All experiments were carried out in buffer containing 10 mM HEPES (pH 7.4), 150 mM NaCl, 3 mM EDTA and 0.05% Tween 20. Ub and Ub chains were injected at concentrations of 0, 2, 4, 10, 25, 50, 100, 200, 400 and 800 µM at a flow rate of 50 µl/min (100 s injections). In case of polyubiquitin chains the concentrations were adjusted according to the number of ubiquitin molecules. Dissociation constants were calculated using the BiaEvaluation software from control-corrected steady-state response units. This yielded apparent dissociation constants for a single ubiquitin within a chain under the assumption that all binding sites are equal.

Cycloheximide Decay Assay

Protein degradation was analyzed in yeast cells by means of blocking translation. 25 OD_{600} of cells in log-phase were suspended in SD medium containing 0.35 mg/ml Cycloheximide and incubated at 30 °C. 500 µl of ice-cold 30 mM NaN_3 and 1mM PMSF stopped degradation after 1, 2 and 3 hours. Cells were lysed by glass beads and strong agitation in 50 mM

Tris/HCl pH 7.5, 1 % (w/v) SDS and 1 mM PMSF. Ubc6, Sec61 and Cue1 were analyzed by SDS-PAGE and Western blotting according to (Bagola et al., 2013).

ACCESSION NUMBERS

Coordinates for the CUE domain structure have been deposited with accession code 2MYX.

SUPPLEMENTAL INFORMATION

Supplemental Information can be found with this article online at.

AUTHOR CONTRIBUTIONS

M.v.D and A.K. designed and performed experiments and wrote the manuscript. V.V.R. and F.L. performed NMR experiments, P.G conducted structure calculation, K.B. and L.P generated constructs and performed experiments. V.V.R., T.S. and V.D. guided the project planning and wrote the manuscript.

ACKNOWLEDGEMENTS

The authors thank Prof. C. Wolberger for Ube1 subcloned in a pET21d vector and all members of the Dötsch and Sommer research group, especially E. Jarosch, for unpublished data, materials and discussions. This work was funded by the Deutsche Forschungsgemeinschaft (SFB 740, Priority Program 1365), the Deutsch-Israelische Projektkooperation (DIP), the LOEWE program, Ubiquitin Networks and the Cluster of Excellence Frankfurt (Macromolecular Complexes). P.G. is supported by a Lichtenberg professorship of the Volkswagen Foundation.

REFERENCES

Bagola, K., Delbrück, M. von, Dittmar, G., Scheffner, M., Ziv, I., Glickman, M.H., Ciechanover, A., and Sommer, T. (2013). Ubiquitin binding by a CUE domain regulates ubiquitin chain formation by ERAD E3 ligases. Mol. Cell *50*, 528–539.

Bays, N.W., Gardner, R.G., Seelig, L.P., Joazeiro, C.A., and Hampton, R.Y. (2001). Hrd1p/Der3p is a membrane-anchored ubiquitin ligase required for ER-associated degradation. Nat. Cell Biol. *3*, 24–29.

Bazirgan, O.A., and Hampton, R.Y. (2008). Cue1p is an activator of Ubc7p E2 activity in vitro and in vivo. J. Biol. Chem. *283*, 12797–12810.

Berndsen, C.E., and Wolberger, C. (2011). A spectrophotometric assay for conjugation of ubiquitin and ubiquitin-like proteins. Anal. Biochem. *418*, 102–110.

Biederer, T., Volkwein, C., and Sommer, T. (1997). Role of Cue1p in ubiquitination and degradation at the ER surface. Science *278*, 1806–1809.

Brown, N.G., Watson, E.R., Weissmann, F., Jarvis, M.A., VanderLinden, R., Grace, Christy R R, Frye, J.J., Qiao, R., Dube, P., Petzold, G., Cho, S.E., Alsharif, O., Bao, J., Davidson, I.F., Zheng, J.J., Nourse, A., Kurinov, I., Peters, J.-M., Stark, H., and Schulman, B.A. (2014). Mechanism of polyubiquitination by human anaphase-promoting complex: RING repurposing for ubiquitin chain assembly. Mol. Cell *56*, 246–260.

Brzovic, P.S., Lissounov, A., Christensen, D.E., Hoyt, D.W., and Klevit, R.E. (2006). A UbcH5/ubiquitin noncovalent complex is required for processive BRCA1-directed ubiquitination. Mol. Cell *21*, 873–880.

Buetow, L., Gabrielsen, M., Anthony, N.G., Dou, H., Patel, A., Aitkenhead, H., Sibbet, G.J., Smith, B.O., and Huang, D.T. (2015). Activation of a primed RING E3-E2-ubiquitin complex by non-covalent ubiquitin. Mol. Cell *58*, 297–310.

Carvalho, P., Goder, V., and Rapoport, T.A. (2006). Distinct ubiquitin-ligase complexes define convergent pathways for the degradation of ER proteins. Cell *126*, 361–373.

Chen, Z.J., and Sun, L.J. (2009). Nonproteolytic functions of ubiquitin in cell signaling. Mol. Cell *33*, 275–286.

Choi, Y.-S., Lee, Y.-J., Lee, S.-Y., Shi, L., Ha, J.-H., Cheong, H.-K., Cheong, C., Cohen, R.E., and Ryu, K.-S. (2014). Differential ubiquitin binding by the acidic loops of Ube2g1 and Ube2r1 distinguishes their K48-ubiquitylation activities. J. Biol. Chem. *290*, 2251-2263.

Choi, Y.-S., Wu, K., Jeong, K., Lee, D., Jeon, Y.H., Choi, B.-S., Pan, Z.-Q., Ryu, K.-S., and Cheong, C. (2010). The human Cdc34 carboxyl terminus contains a non-covalent ubiquitin binding activity that contributes to SCF-dependent ubiquitination. J. Biol. Chem. *285*, 17754–17762.

Conaway, R.C., Brower, C.S., and Conaway, J.W. (2002). Emerging roles of ubiquitin in transcription regulation. Science *296*, 1254–1258.

Crosas, B., Hanna, J., Kirkpatrick, D.S., Zhang, D.P., Tone, Y., Hathaway, N.A., Buecker, C., Leggett, D.S., Schmidt, M., King, R.W., Gygi, S.P., and Finley, D. (2006). Ubiquitin chains

are remodeled at the proteasome by opposing ubiquitin ligase and deubiquitinating activities. Cell *127*, 1401–1413.

de Vries, Sjoerd J, van Dijk, M., and Bonvin, Alexandre M J J (2010). The HADDOCK web server for data-driven biomolecular docking. Nat. Prot. *5*, 883–897.

Denic, V., Quan, E.M., and Weissman, J.S. (2006). A luminal surveillance complex that selects misfolded glycoproteins for ER-associated degradation. Cell *126*, 349–359.

Foresti, O., Rodriguez-Vaello, V., Funaya, C., and Carvalho, P. (2014). Quality control of inner nuclear membrane proteins by the Asi complex. Science *346*, 751–755.

Haglund, K., and Dikic, I. (2005). Ubiquitylation and cell signaling. EMBO J. *24*, 3353–3359.

Huang, T.T., and D'Andrea, A.D. (2006). Regulation of DNA repair by ubiquitylation. Nat. Rev. Mol. Cell Biol. *7*, 323–334.

Husnjak, K., and Dikic, I. (2012). Ubiquitin-binding proteins: decoders of ubiquitin-mediated cellular functions. Ann. Rev. Biochem. *81*, 291–322.

Jentsch, S., and Rumpf, S. (2007). Cdc48 (p97): a "molecular gearbox" in the ubiquitin pathway? Trends in Biochemical Sciences *32*, 6–11.

Kang, R.S., Daniels, C.M., Francis, S.A., Shih, S.C., Salerno, W.J., Hicke, L., and Radhakrishnan, I. (2003). Solution structure of a CUE-ubiquitin complex reveals a conserved mode of ubiquitin binding. Cell *113*, 621–630.

Kelly, A., Wickliffe, K.E., Song, L., Fedrigo, I., and Rape, M. (2014). Ubiquitin chain elongation requires E3-dependent tracking of the emerging conjugate. Mol. Cell *56*, 232–245.

Khmelinskii, A., Blaszczak, E., Pantazopoulou, M., Fischer, B., Omnus, D.J., Le Dez, G., Brossard, A., Gunnarsson, A., Barry, J.D., Meurer, M., Kirrmaier, D., Boone, C., Huber, W., Rabut, G., Ljungdahl, P.O., and Knop, M. (2014). Protein quality control at the inner nuclear membrane. Nature *516*, 410–413.

Koegl, M., Hoppe, T., Schlenker, S., Ulrich, H.D., Mayer, T.U., and Jentsch, S. (1999). A novel ubiquitination factor, E4, is involved in multiubiquitin chain assembly. Cell *96*, 635–644.

Komander, D., and Rape, M. (2012). The ubiquitin code. Ann. Rev Biochem. *81*, 203–229.

Kostova, Z., Mariano, J., Scholz, S., Koenig, C., and Weissman, A.M. (2009). A Ubc7p-binding domain in Cue1p activates ER-associated protein degradation. J. Cell Science *122*, 1374–1381.

Kreft, S.G., and Hochstrasser, M. (2011). An unusual transmembrane helix in the endoplasmic reticulum ubiquitin ligase Doa10 modulates degradation of its cognate E2 enzyme. J. Biol. Chem. *286*, 20163–20174.

Kreft, S.G., Wang, L., and Hochstrasser, M. (2006). Membrane topology of the yeast endoplasmic reticulum-localized ubiquitin ligase Doa10 and comparison with its human ortholog TEB4. J. Biol. Chem. *281*, 4646–4653.

Liu, S., Chen, Y., Li, J., Huang, T., Tarasov, S., King, A., Weissman, A.M., Byrd, R.A., and Das, R. (2012). Promiscuous interactions of gp78 E3 ligase CUE domain with polyubiquitin chains. Structure *20*, 2138–2150.

Mansour, W., Nakasone, M.A., Delbrueck, M. von, Yu, Z., Krutauz, D., Reis, N., Kleifeld, O., Sommer, T., Fushman, D., and Glickman, M.H. (2014). Disassembly of Lys11- and mixed-linkage polyubiquitin conjugates provide insights into function of proteasomal deubiquitinases Rpn11 and Ubp6. J. Biol. Chem. *290*, 4688-4704.

Metzger, M.B., Liang, Y.-H., Das, R., Mariano, J., Li, S., Li, J., Kostova, Z., Byrd, R.A., Ji, X., and Weissman, A.M. (2013). A structurally unique E2-binding domain activates ubiquitination by the ERAD E2, Ubc7p, through multiple mechanisms. Mol. Cell *50*, 516–527.

Meyer, H.-J., and Rape, M. (2014). Enhanced protein degradation by branched ubiquitin chains. Cell *157*, 910–921.

Pastushok, L., Moraes, T.F., Ellison, M.J., and Xiao, W. (2005). A single Mms2 "key" residue insertion into a Ubc13 pocket determines the interface specificity of a human Lys63 ubiquitin conjugation complex. J. Biol. Chem. *280*, 17891–17900.

Pickart, C.M., and Raasi, S. (2005). Controlled synthesis of polyubiquitin chains. Meth. Enzymol. *399*, 21–36.

Ravid, T., and Hochstrasser, M. (2007). Autoregulation of an E2 enzyme by ubiquitin-chain assembly on its catalytic residue. Nat. Cell Biol. *9*, 422–427.

Rogov, V.V., Rozenknop, A., Rogova, N.Y., Löhr, F., Tikole, S., Jaravine, V., Güntert, P., Dikic, I., and Dötsch, V. (2012). A universal expression tag for structural and functional studies of proteins. Chembiochem *13*, 959–963.

Schmidt, M., Hanna, J., Elsasser, S., and Finley, D. (2005). Proteasome-associated proteins: regulation of a proteolytic machine. Biol. Chem. *386*, 725–737.

Thrower, J.S., Hoffman, L., Rechsteiner, M., and Pickart, C.M. (2000). Recognition of the polyubiquitin proteolytic signal. EMBO J. *19*, 94–102.

Varadan, R., Assfalg, M., Raasi, S., Pickart, C., and Fushman, D. (2005). Structural determinants for selective recognition of a Lys48-linked polyubiquitin chain by a UBA domain. Mol. Cell *18*, 687–698.

Wang, Z.X., and Jiang, R.F. (1996). A novel two-site binding equation presented in terms of the total ligand concentration. FEBS Lett. *392*, 245–249.

Weissman, A.M. (2001). Themes and variations on ubiquitylation. Nat. Rev. Mol. Cell Biol. *2*, 169–178.

Wickliffe, K.E., Lorenz, S., Wemmer, D.E., Kuriyan, J., and Rape, M. (2011). The mechanism of linkage-specific ubiquitin chain elongation by a single-subunit E2. Cell *144*, 769–781.

Wright, J.D., Mace, P.D., and Day, C.L. (2016). Secondary ubiquitin-RING docking enhances Arkadia and Ark2C E3 ligase activity. Nat. Struc. & Mol. Biol. *23*, 45–52.

Xu, P., Duong, D.M., Seyfried, N.T., Cheng, D., Xie, Y., Robert, J., Rush, J., Hochstrasser, M., Finley, D., and Peng, J. (2009). Quantitative proteomics reveals the function of unconventional ubiquitin chains in proteasomal degradation. Cell *137*, 133–145.

FIGURE LEGENDS

Figure 1: The interaction of the CUE domain with ubiquitin and fluorescence anisotropy-based analysis of ubiquitin chain elongation reactions

(A) Superposition of the NMR solution structure (PDB code: 2MYX) ensemble comprising the 20 lowest energy conformers. The three α-helices are colored in yellow, green and cyan (from N to C terminus), whereas the structured regions following and preceding the three helices are colored in blue (C-terminal extension) and red (N-terminal extension). The LAP motif is highlighted in orange. See also Figure S1a.

(B) Mapping of affected residues upon binding onto the structure of the CUE domain and ubiquitin (PDB code: 1UBQ). The structures are shown as a ribbon diagram as well as a surface representation. Residues shifting more than 0.12 ppm are colored in yellow and residues shifting more than 0.18 ppm in red for Cue1. For ubiquitin, residues shifting more than 0.13 ppm are shown in yellow, whereas residues shown in red shifted more than 0.22 ppm. See also Figure S1b.

(C) Model of the CUE/ubiquitin complex. The highest scored structural model from a CSP-based HADDOCK structure calculation is shown. The structure reveals the importance of R42 of ubiquitin for complex formation. CUE is bound in close proximity to the K48 residue, the site of further chain conjugation, however, K48 itself remains completely accessible.

(D) Ubiquitin chains are elongated *in vitro* by one ubiquitin moiety. Due to a C-terminal His_6-tag preassembled chains only serve as an acceptor for ubiquitin. Fluorescently labeled ubiquitin is activated by the E1 enzyme and transferred to the E2 enzyme Ubc7. In concert with the cytosolic fragment of Cue1 (cCue1) Ubc7 elongates ubiquitin chains that are employed in excess. The RING domain of Hrd1 (cHrd1) is optionally added to facilitate the reaction. See also Figure S1c.

(E) In fluorescence anisotropy measurements a rising signal monitors the elongation of K48-linked tetraubiquitin (—). After subsequent addition of a deubiquitinating enzyme ($Usp2_{cat}$) anisotropy signals decrease (—) close to the baseline of reactions omitting ATP (—). Reactions lacking ATP or preassembled ubiquitin chains (—) do not show an increase in anisotropy.

(F) The yield of elongation products was determined by SDS-PAGE, fluorescence scanning and Coomassie staining. Added $Usp2_{cat}$ is marked with an asterisk (*).

Figure 2: The ubiquitin binding affinity of the CUE domain correlates with the kinetics of ubiquitin chain elongation reactions *in vitro* and the degradation of the ERAD-substrate Ubc6 *in vivo*.

(A) Superposition of a section of [^{15}N, ^{1}H]-HSQC spectra recorded for cCue1 variants E96A, E100A, L103A in presence (8-fold molar excess of ubiquitin ●) and absence of ubiquitin (●). As a reference the spectrum recorded for the wild type CUE domain in presence of the same amount of ubiquitin is shown (●) (See also Figure S2). Binding of the E96A variant resembles the wild type protein, while variants E100A and L103A show diminished affinities. Substitutions in the LAP motif L76R A77G P78A (cCue1 RGA) result in an unfolded CUE domain (Figure S1a F) and prevent an interaction with ubiquitin.

Fluorescence anisotropy traces were obtained from K48-Ub_4 elongation reactions with Ubc7 and cCue1 (—) or cCue1 variants (E96A —, E100A —, L103A —, RGA —) in presence (B) or absence of cHrd1 (C). Solid lines show monoexponential fits of the data points on which basis kinetic parameters were calculated.

(D) Rate constants of elongation reactions of tetraubiquitin with cCue1 or variants in (B).

(E) Chemical shift perturbations (CSPs) of representative residues (V73, L76, A77) upon ubiquitin binding. Obtained shifts at 8-fold molar excess of ubiquitin are compared between

wildytpe and CUE domain variants. The ratio between the CSPs observed for the wildtype CUE domain and its variants was calculated.

(F) The yield of assembled elongation product pentaubiquitin of reactions in (B) is calculated by the ratio of fluorescent pentaubiquitin over non-conjugated fluorescently-labeled monoubiquitin.

(G) Quantification of a cycloheximide based decay assay of Ubc6 performed in presence of the Cue1 variants (Figure S2C). The kinetics of degradation are color-coded as in B. The quantities of variant proteins were similar throughout the experiments. Remaining amounts of Ubc6 from Δcue1 and Δubc7 strains (data from a separate experiment) provide a baseline and indicate maximal delay of Ubc6 degradation.

Figure 3: The CUE domain of Cue1 preferentially binds K48-linked ubiquitin chains and stimulates their elongation.

(A) Kinetics of monoubiquitin (—) and diubiquitin (---) elongation by Ubc7 and cCue1 (—) or cCue1 RGA (—) monitored by time course experiments. The CUE domain stimulates elongation of ubiquitin chains but not of monoubiquitin.

(B) Kinetic rate constants of elongation reactions with cCue1 and Ubc7 for a set of ubiquitin chains linked *via* K48 or K63 (Figure S3 A-F). K63-linked model substrates are restricted for distal elongation by K48R ubiquitin variants except at the distal moiety. Reactions accelerate from top to bottom with K48-Ub_4 elongated fastest.

(C) K_D values for the interaction between the CUE domain and different ubiquitin chains were calculated from SPR binding data assuming a 1:1 binding model with multiple, independent and equal binding sites.

(D) Kinetic rate constants of elongation reactions with Ubc7, cHrd1 and cCue1 (■) or cCue1 RGA (■) are shown in comparison for different substrate chains.

(E) Acceleration factors which quantify the CUE specific stimulation were calculated as a ratio of kinetic rate constants of reactions with wild type Cue1 and rate constants of reactions with Cue1 RGA (■). The stimulating effect of the CUE domain is most pronounced for K48-linked chains and rises with increasing chain length for this linkage type.

(F) A working model of cCue1/Ubc7 illustrates ubiquitin chain elongation in presence and absence of CUE domain´s binding activity.

Figure 4: The CUE domain preferentially binds the proximal moiety in K48-linked diubiquitin

(A) Backbone amide CSP mapping of ^{15}N-labeled proximal ubiquitin or ^{15}N-labeled distal ubiquitin in K48-Ub_2 upon titration with unlabeled CUE domain. Proximal ubiquitin and the resulting CSPs are colored blue, distal ubiquitin and the corresponding CSPs red. Since the backbone amide signal of R42 disappeared the indicated CSP of R42 was set to the arbitrary value of 0.5 to emphasize its importance in mediating CUE recognition. The CSP of G75 in distal ubiquitin is colored in blue because we propose that this represents an additional interaction with proximally bound CUE.

(B) The same data as in A for K63-Ub_2.

(C) Overlay of a representative section of the [^{15}N, ^{1}H]-HSQC spectra showing the unbound form of proximal/distal ubiquitin in black and the spectra recorded at a 1:1 molar ratio of CUE:Ub_2 either with proximally (blue) or distally (red) ^{15}N-labeled samples. Larger shifts for proximal ubiquitin indicate a significantly higher population of proximally bound CUE.

(D) The same overlays as in C for K63-Ub_2. CUE interactions with proximal and distal ubiquitin of K63-Ub_2 are similar.

(E, F) Determination of K_D values from the CSP data. The data was fitted assuming a binding model with two independent but different binding sites. The fit reveals a two fold increase in affinity for proximal K48-linked ubiquitin. See also Figure S4.

Figure 5: An interaction of the CUE domain with the moiety adjacent to the distal acceptor ubiquitin strongly promotes chain elongation.

(A) Elongation of diubiquitin catalyzed by Ubc7 and cCue1 (—) or cCue1 RGA (—) was followed by time course experiments. The kinetics of reactions with wild type diubiquitin (●) and a variant with distal R42A ubiquitin (▼) were similar in presence of cCue1. In contrast, the elongation of diubiquitin containing a proximal R42A ubiquitin was significantly decelerated (■). Reactions with this set of diubiquitin molecules and cCue1 RGA exhibited almost identical kinetics.

(B) Kinetic rate constants of elongation reactions with cCue1, Ubc7 and K48-Ub_4 variants bearing single R42A ubiquitin molecules (Figure S5B, S5D). Deceleration of chain elongation is most pronounced for R42A that is located in the moiety adjacent to the distal acceptor ubiquitin. cCue1 binding at this position in tetraubiquitin as well as distal chain elongation by Ubc7 are schematically depicted in our working model.

(C) Kinetic rate constants of reactions with cCue1, Ubc7 and K48-Ub_4 variants that contain multiple R42A substitutions. An increasing number of substitutions progressively decelerates elongation kinetics (Figure S5C, S5E).

(D) Elongation reactions with cCue1 T66C C147S crosslinked to Ub T9C which is placed at different positions in ubiquitin chains are monitored by time course experiments. Crosslinking cCue1 to the distal position of K48-linked diubiquitin (K48-Ub_2^{distal}~cCue1, —) strongly decelerates elongation. cCue1 fixed at proximal sites of di- (K48-$Ub_2^{proximal}$~cCue1, —) or triubiquitin (K48-$Ub_3^{proximal}$~cCue1, —) yields fast kinetics. Reactions without crosslinking were performed with equimolar amounts of cCue1 and K48-Ub_2 (—)as a reference. See also Figure S5 F-G.

Figure 6: Model of the Cue1-CUE domain-assisted ubiquitin chain assembly by Ubc7

The CUE domain of Cue1 binds single moieties of ubiquitin chains and aligns the E2 Ubc7 with the distal end of the polymer. Binding events adjacent to the acceptor ubiquitin promote chain elongation most. In addition, longer chains keep the E2 enzyme in close proximity to the acceptor ubiquitin.

Figure 1:

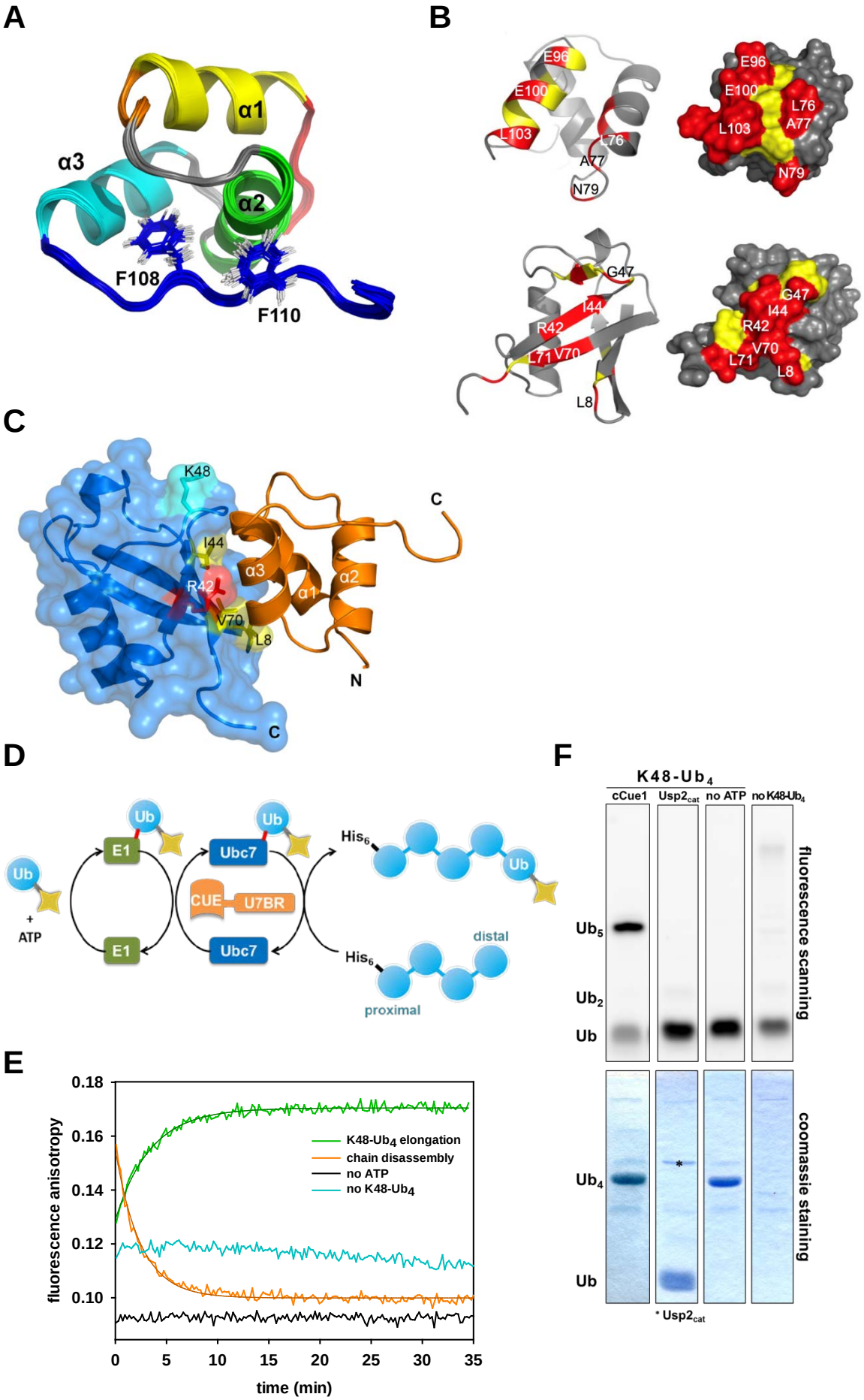
A
α1
α3
α2
F108
F110
B
E96
E100
L103
L76
A77
N79
G47
I44
R42
L71
V70
L8
C
K48
I44
R42
V70
L8
α3
α1
α2
C
N
C
D
Ub
E1
Ubc7
CUE
U7BR
ATP
His6
distal
proximal
E
fluorescence anisotropy
0.18
0.16
0.14
0.12
0.10
0
5
10
15
20
25
30
35
time (min)
K48-Ub4 elongation
chain disassembly
no ATP
no K48-Ub4
F
K48-Ub4
cCue1
Usp2cat
no ATP
no K48-Ub4
Ub5
Ub2
Ub
Ub4
Ub
* Usp2cat
fluorescence scanning
coomassie staining

Figure 2:

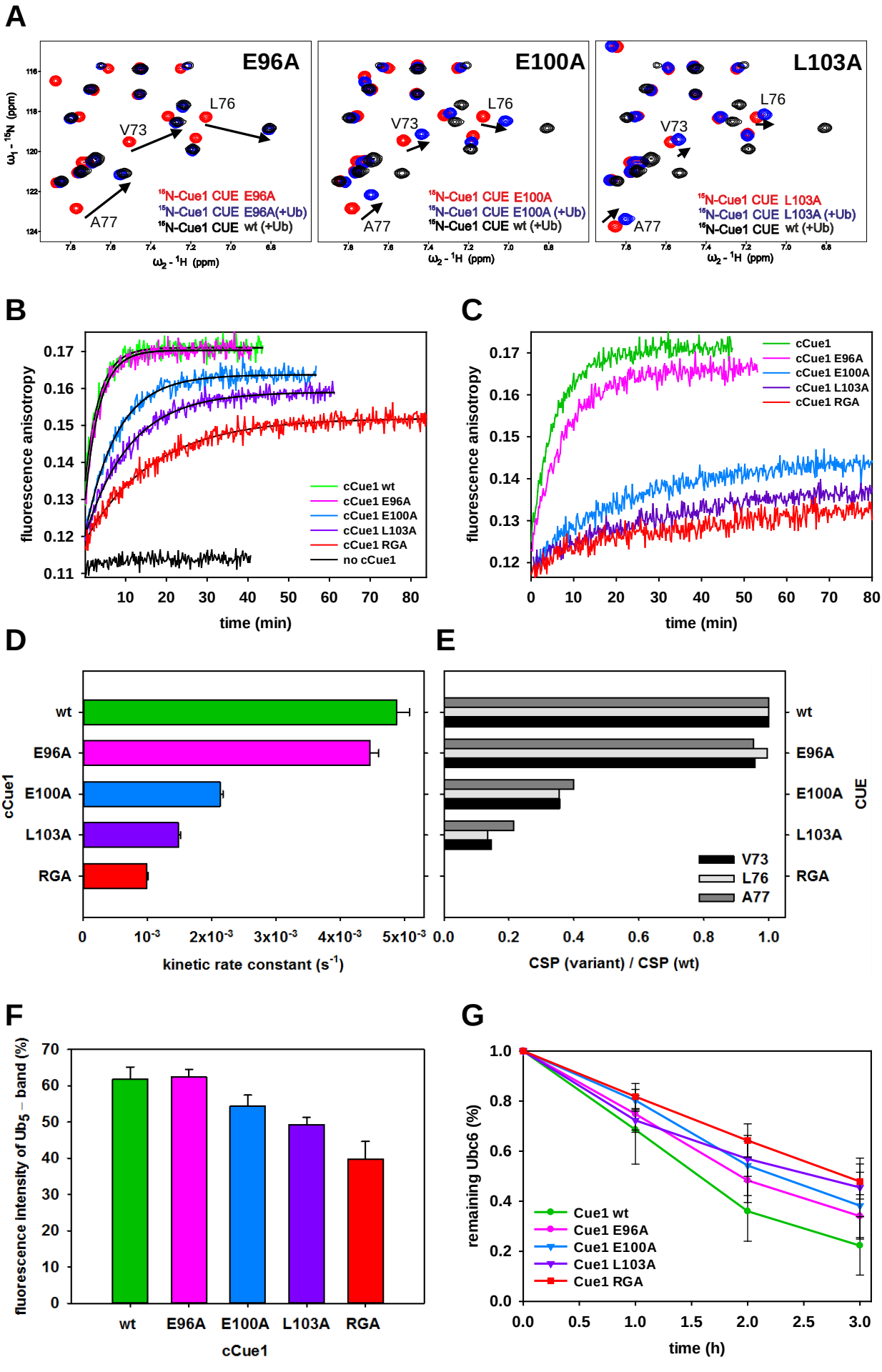
A
E96A
E100A
L103A
L76
V73
A77
^{15}N-Cue1 CUE E96A
^{15}N-Cue1 CUE E96A(+Ub)
^{15}N-Cue1 CUE wt (+Ub)
^{15}N-Cue1 CUE E100A
^{15}N-Cue1 CUE E100A (+Ub)
^{15}N-Cue1 CUE wt (+Ub)
^{15}N-Cue1 CUE L103A
^{15}N-Cue1 CUE L103A (+Ub)
^{15}N-Cue1 CUE wt (+Ub)
ω_1 - ^{15}N (ppm)
ω_2 - ^{1}H (ppm)
B
fluorescence anisotropy
time (min)
cCue1 wt
cCue1 E96A
cCue1 E100A
cCue1 L103A
cCue1 RGA
no cCue1
C
cCue1
cCue1 E96A
cCue1 E100A
cCue1 L103A
cCue1 RGA
D
cCue1
wt
E96A
E100A
L103A
RGA
kinetic rate constant (s^{-1})
E
CUE
V73
L76
A77
CSP (variant) / CSP (wt)
F
fluorescence intensity of Ub_5 – band (%)
cCue1
G
remaining Ubc6 (%)
time (h)
Cue1 wt
Cue1 E96A
Cue1 E100A
Cue1 L103A
Cue1 RGA

Figure 3:

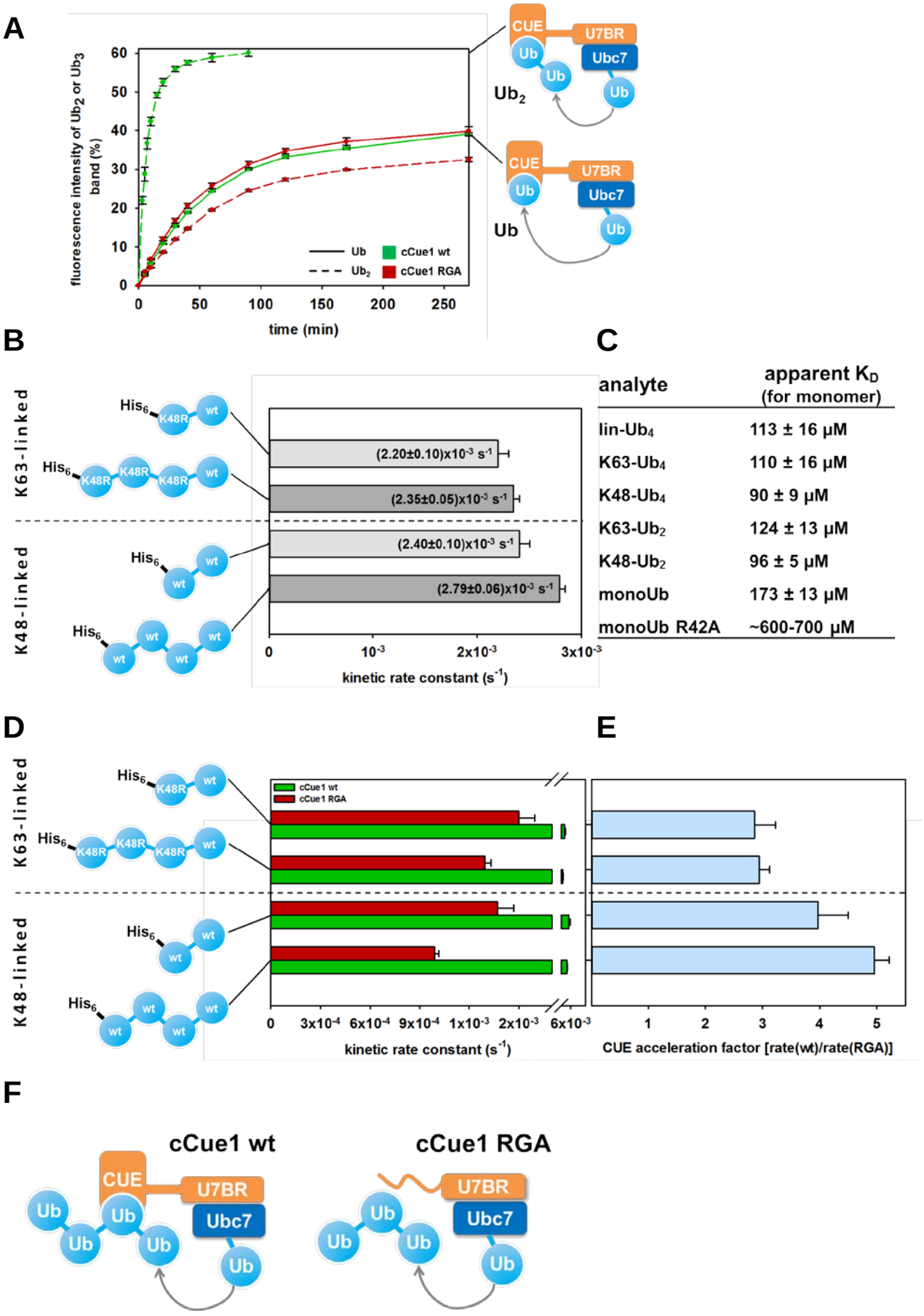
A
fluorescence intensity of Ub2 or Ub3 band (%)
time (min)
Ub
Ub2
cCue1 wt
cCue1 RGA
CUE
U7BR
Ubc7
Ub
B
K63-linked
K48-linked
His6
K48R
wt
(2.20±0.10)x10-3 s-1
(2.35±0.05)x10-3 s-1
(2.40±0.10)x10-3 s-1
(2.79±0.06)x10-3 s-1
kinetic rate constant (s-1)
C
analyte
apparent KD (for monomer)
lin-Ub4 113 ± 16 µM
K63-Ub4 110 ± 16 µM
K48-Ub4 90 ± 9 µM
K63-Ub2 124 ± 13 µM
K48-Ub2 96 ± 5 µM
monoUb 173 ± 13 µM
monoUb R42A ~600-700 µM
D
E
CUE acceleration factor [rate(wt)/rate(RGA)]
F
cCue1 wt
cCue1 RGA

Figure 4:

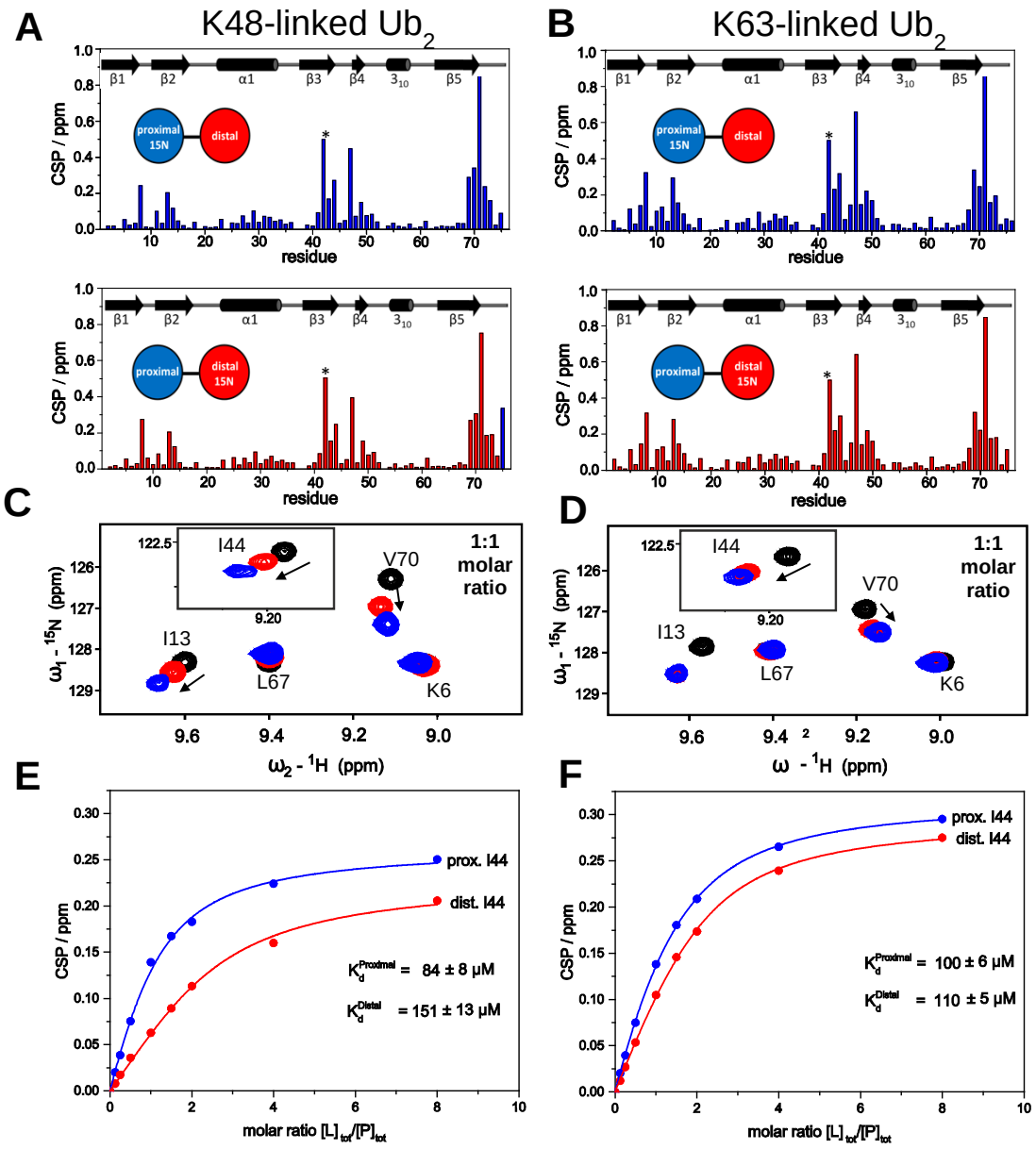
A
K48-linked Ub2
B
K63-linked Ub2
CSP / ppm
residue
proximal 15N
distal
proximal
distal 15N
C
D
1:1 molar ratio
I44
V70
I13
L67
K6
ω1 - 15N (ppm)
ω2 - 1H (ppm)
E
F
prox. I44
dist. I44
Kd Proximal = 84 ± 8 µM
Kd Distal = 151 ± 13 µM
Kd Proximal = 100 ± 6 µM
Kd Distal = 110 ± 5 µM
molar ratio [L]tot/[P]tot

Figure 5:

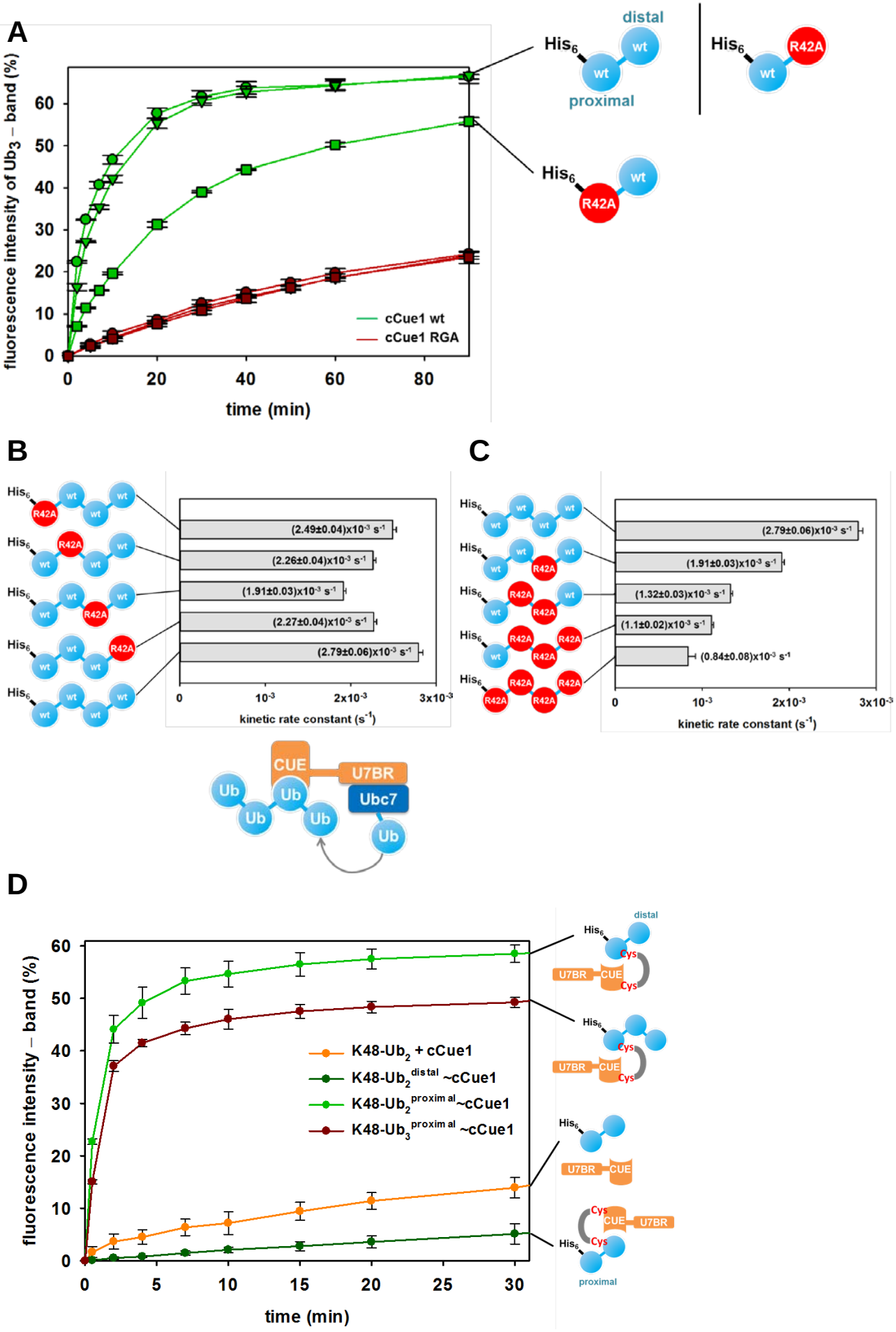
A
fluorescence intensity of Ub3 – band (%)
time (min)
cCue1 wt
cCue1 RGA
distal
proximal
His6
wt
R42A
B
(2.49±0.04)x10-3 s-1
(2.26±0.04)x10-3 s-1
(1.91±0.03)x10-3 s-1
(2.27±0.04)x10-3 s-1
(2.79±0.06)x10-3 s-1
kinetic rate constant (s-1)
C
(2.79±0.06)x10-3 s-1
(1.91±0.03)x10-3 s-1
(1.32±0.03)x10-3 s-1
(1.1±0.02)x10-3 s-1
(0.84±0.08)x10-3 s-1
kinetic rate constant (s-1)
CUE
U7BR
Ubc7
Ub
D
fluorescence intensity – band (%)
time (min)
K48-Ub2 + cCue1
K48-Ub2distal ~cCue1
K48-Ub2proximal ~cCue1
K48-Ub3proximal ~cCue1
distal
proximal
Cys

Figure 6:

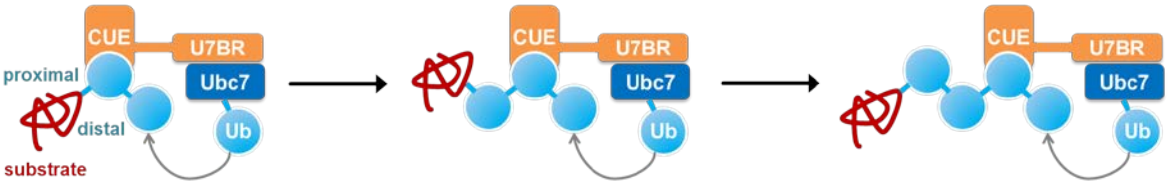
CUE
U7BR
proximal
Ubc7
distal
Ub
substrate
CUE
U7BR
Ubc7
Ub
CUE
U7BR
Ubc7
Ub